Protein mutants and transient transfections

We used the following protein mutants: RLIMΔ9 (residues 562–571 in the RING finger are deleted), RLIMΔRING (1–543), CLIM2ΔC (1–271), Lhx3ΔC (1–266), and proteins CLIM1, CLIM2 (ref. 21) and LMO2-LIM, RLIM, N-RLIM (1–207), M-RLIM (208–423), C-RLIM (403–600), DN-CLIM (225–341)[8]. Transient transfections and co-transfections were carried out using a Superfect transfection kit (Qiagen), as described previously[23].

Immunocytochemistry and RNAi

RNAi experiments were performed as reported[24], transfecting HeLa cells with double-stranded RNA oligonucleotides (Dharmacon) containing human RLIM sequences[20], or with a single-strand sense control (sequence information available on request) using the Oligofectamine kit (Invitrogen). Cells were visualized with RLIM or CLIM antisera and Toto-3 dye (Molecular Probes). In parallel experiments, protein levels of transfected cells were monitored by western blots using RLIM or CLIM antisera. Immunostainings of transfected cells were performed as reported[25]. The experiments were analysed and pictures taken on a confocal microscope (Leica DMIRBE).

Protein–protein interactions and EMSA experiments

The *in vitro* protein–protein interaction experiments were carried out with bacterially expressed GST fusion proteins and ^{35}S-labelled proteins produced by *in vitro* transcription/translation using a TNT *in vitro* translation kit (Promega), as described[23], with the modification that all binding and washing steps were carried out at 37 °C. For ubiquitinations in EMSA, bacterially expressed proteins and ^{32}P-labelled oligonucleotides containing the LIM-HD recognition site in the αGSU promoter[23,26] were incubated for 10 min on ice, as described[8,21], in buffer[27] supplemented with 4 mM ATP and 8 mM $MgCl_2$. Subsequently, E1, UbcH5 and ubiquitin were added, followed by a 2 h incubation at 30 °C.

Chromatin immunoprecipitation assays

ChIP assays were essentially done as described[3], using anti-Lhx3/Plim[21], anti-CLIM, anti-RLIM, and anti-Myc (BabCo) antisera, and oligonucleotides encompassing the region on the mouse αGSU promoter that contains the LIM-HD binding site[23,26] (see Supplementary Information).

Received 12 October 2001; accepted 17 January 2002.

1. Mannervik, M., Nibu, Y., Zhang, H. & Levine, M. Transcriptional coregulators in development. *Science* **284,** 606–609 (1999).
2. Glass, C. K. & Rosenfeld, M. G. The coregulator exchange in transcriptional functions of nuclear receptors. *Genes Dev.* **14,** 121–141 (2000).
3. Shang, Y., Hu, X., DiRenzo, J., Lazar, M. A. & Brown, M. Cofactor dynamics and sufficiency in estrogen receptor-regulated transcription. *Cell* **103,** 843–852 (2000).
4. Bach, I. The LIM domain: regulation by association. *Mech. Dev.* **91,** 5–17 (2000).
5. Hobert, O. & Westphal, H. Functions of LIM homeobox genes. *Trends Genet.* **16,** 75–83 (2000).
6. Agulnick, A. D. *et al.* Interactions of the LIM-domain-binding factor Ldb1 with LIM homeodomain proteins. *Nature* **384,** 270–272 (1996).
7. Morcillo, P., Rosen, C., Baylies, M. K. & Dorsett, D. Chip, a widely expressed chromosomal protein required for segmentation and activity of a remote wing margin enhancer in *Drosophila*. *Genes Dev.* **11,** 2729–2740 (1997).
8. Bach, I. *et al.* RLIM inhibits functional activity of LIM homeodomain transcription factors via recruitment of the histone deacetylase complex. *Nature Genet.* **22,** 394–399 (1999).
9. Milán, M. & Cohen, S. M. Regulation of LIM homeodomain activity *in vivo*: a tetramer of dLDB and Apterous confers activity and capacity for regulation by dLMO. *Mol. Cell* **4,** 267–273 (1999).
10. van Meyel, D. J. *et al.* Chip and Apterous physically interact to form a functional complex during *Drosophila* development. *Mol. Cell* **4,** 259–265 (1999).
11. van Meyel, D. J. *et al.* Chip is an essential cofactor for Apterous in the regulation of axon guidance in *Drosophila*. *Development* **127,** 1823–1831 (2000).
12. Milán, M., Diaz-Benjumea, F. J. & Cohen, S. M. Beadex encodes an LMO protein that regulates Apterous LIM-homeodomain activity in *Drosophila* wing development: a model for LMO oncogene function. *Genes Dev.* **12,** 2912–2920 (1998).
13. Hershko, A. & Ciechanover, A. The ubiquitin system. *Annu. Rev. Biochem.* **67,** 425–479 (1998).
14. Tiedt, R., Bartholdy, B. A., Matthias, G., Newell, J. W. & Matthias, P. The RING finger protein Siah-1 regulates the level of the transcriptional coactivator OBF-1. *EMBO J.* **20,** 4143–4152 (2001).
15. Boehm, J., He, Y., Greiner, A., Staudt, L. & Wirth, T. Regulation of BOB.1/OBF-1 stability by SIAH. *EMBO J.* **20,** 4153–4162 (2001).
16. Joazeiro, C. A. P. & Weissman, A. M. RING finger proteins: mediators of ubiquitin ligase activity. *Cell* **79,** 549–552 (2000).
17. Pickart, C. M. Mechanisms underlying ubiquitination. *Annu. Rev. Biochem.* **70,** 503–533 (2001).
18. Lorick, K. L. *et al.* RING fingers mediate ubiquitin-conjugating enzyme (E2)-dependent ubiquitination. *Proc. Natl Acad. Sci. USA* **96,** 11364–11369 (1999).
19. Windle, J. J., Weiner, R. I. & Mellon, P. L. Cell lines of the pituitary gonadotrope lineage derived by targeted oncogenesis in transgenic mice. *Mol. Endocrinol.* **4,** 597–603 (1990).
20. Ostendorff, H. P. *et al.* Functional characterization of the gene encoding RLIM, the corepressor of LIM homeodomain factors. *Genomics* **69,** 120–130 (2000).
21. Bach, I., Carrière, C., Ostendorff, H. P., Andersen, B. & Rosenfeld, M. G. A family of LIM domain interacting cofactors confer transcriptional synergism between LIM and Otx homeoproteins. *Genes Dev.* **11,** 1370–1380 (1997).
22. Jurata, L. W. & Gill, G. N. Functional analysis of the nuclear LIM domain interactor NLI. *Mol. Cell Biol.* **17,** 5688–5698 (1997).
23. Bach, I. *et al.* P-Lim, a LIM homeodomain factor, is expressed during pituitary organ and cell commitment and synergizes with Pit-1. *Proc. Natl Acad. Sci. USA* **92,** 2720–2724 (1995).
24. Elbashir, S. M. *et al.* Duplexes of 21-nucleotide RNAs mediate RNA interference in cultured mammalian cells. *Nature* **411,** 494–498 (2001).
25. Bach, I. & Yaniv, M. More potent transcriptional activators or a transdominant inhibitor of the HNF1 homeoprotein family are generated by alternative RNA processing. *EMBO J.* **12,** 4229–4242 (1993).
26. Roberson, M. S., Schoderbek, W. E., Tremml, G. & Maurer, R. A. Activation of the glycoprotein hormone α-subunit promoter by a LIM-homeodomain transcription factor. *Mol. Cell. Biol.* **14,** 2985–2993 (1994).
27. Yu, V. C. *et al.* RXR β: a coregulator that enhances binding of retinoic acid, thyroid hormone, and vitamin D receptors to their cognate response elements. *Cell* **67,** 1251–1266 (1991).

Supplementary Information accompanies the paper on *Nature*'s website (http://www.nature.com).

Acknowledgements

We thank P. Mellon for the gift of αT3 cells; A. Krones and Y. Alvarez for advice on ChIP assays and chick electroporations, respectively; T. Heinzel for Sin3 expression vectors; I. Hermans-Borgmeyer for comments on the manuscript; and Y. Bodingbauer for technical assistance. H.P.O. was a fellow of the Graduiertenkolleg 255 of the University of Hamburg, and I.B. is a Heisenberg scholar of the Deutsche Forschungsgemeinschaft (DFG). I.B. and M.S. are supported by grants from the DFG.

Competing interests statement

The authors declare that they have no competing financial interests.

Correspondence and requests for materials should be addressed to I.B. (e-mail: ingolf.bach@zmnh.uni-hamburg.de).

Structure of the HP1 chromodomain bound to histone H3 methylated at lysine 9

Peter R. Nielsen*, Daniel Nietlispach*, Helen R. Mott*, Juliana Callaghan*, Andrew Bannister†, Tony Kouzarides†, Alexey G. Murzin‡, Natalia V. Murzina* & Ernest D. Laue*

** Cambridge Centre for Molecular Recognition, Department of Biochemistry, University of Cambridge, 80 Tennis Court Road, Cambridge CB2 1GA, UK*
† Wellcome/Cancer Research UK, Institute of Cancer and Developmental Biology and Department of Pathology, University of Cambridge, Tennis Court Road, Cambridge CB2 1QR, UK
‡ MRC Centre for Protein Engineering, Hills Road, Cambridge CB2 2QH, UK

Specific modifications to histones are essential epigenetic markers[1]—heritable changes in gene expression that do not affect the DNA sequence. Methylation of lysine 9 in histone H3 is recognized by heterochromatin protein 1 (HP1), which directs the binding of other proteins to control chromatin structure and gene expression[2–4]. Here we show that HP1 uses an induced-fit mechanism for recognition of this modification, as revealed by the structure of its chromodomain bound to a histone H3 peptide dimethylated at Nζ of lysine 9. The binding pocket for the *N*-methyl groups is provided by three aromatic side chains, Tyr 21, Trp 42 and Phe 45, which reside in two regions that become ordered on binding of the peptide. The side chain of Lys 9 is almost fully extended and surrounded by residues that are conserved in many other chromodomains. The QTAR peptide sequence preceding Lys 9 makes most of the additional interactions with the chromodomain, with HP1 residues Val 23, Leu 40, Trp 42, Leu 58 and Cys 60 appearing to be a major determinant of specificity by binding the key buried Ala 7. These findings predict which other chromodomains will bind methylated proteins and suggest a motif that they recognize.

Histone methylation is important in the regulation of chromatin structure and thus gene expression[5]. Methylation at lysine 9 of histone H3 by Suv39 methyltransferase[6] and its relatives strongly

correlates with a repressed chromatin state[7,8]. Transcriptional repression through Lys 9 methylation has been demonstrated at centromeric heterochromatin in yeast[2,4] and at retinoblastoma-regulated promoters in mammalian cells[9]. This repression requires the specific recognition of Lys 9-methylated histone H3 by the HP1 chromodomain[2,3].

The structure of the free chromodomain of mouse HP1β (also known as MOD1 or M31)[10] provided no clue as to the mechanism of its recognition of methyl lysine. Methylation of DNA is known to control protein–nucleic acid interactions in many biological systems, but how protein methylation promotes protein–protein interactions is unknown. There is no precedent for the molecular recognition of a lysine residue modified with a variable number of extra methyl groups at the end of its flexible side chain. Unlike acetylation, methylation neither introduces new hydrogen-bonding opportunities nor changes the net charge, so there can be no contribution from additional hydrogen bonds and/or electrostatic interactions. The mechanism of methyl lysine recognition by the HP1 chromodomain thus has wide implications for our understanding of molecular and structural biology. To understand methyl lysine recognition, and to illuminate the role of other chromodomains, we determined the structure of the HP1β chromodomain–histone H3 peptide complex (Fig. 1).

In the complex, the chromodomain adopts the canonical fold found previously in the free and shadow chromodomains[10–13]. The histone H3 peptide binds in an extended β-strand-like conformation in the groove predicted previously[10], using an induced-fit mechanism for recognition of the methylated peptide (Fig. 1a, b). The amino-terminal tail of the free chromodomain wraps around the peptide as it binds (Fig. 1c). This brings together the side chains of three conserved aromatic residues, Tyr 21, Trp 42 and Phe 45, which bind the methyl groups of dimethyl lysine 9 in a pocket formed by their mutually orthogonal aromatic rings (Fig. 2a). The positions of the methyl lysine and interacting chromodomain residues are all well determined by the nuclear magnetic resonance (NMR) data, but there is space for one more methyl group in this pocket, and trimethyl lysine binds similarly (the dissociation constant K_d for the dimethylated and trimethylated peptides are 2.1 and 1.9 μM, respectively). It is significant that aromatic rather than aliphatic residues are used for the recognition of the methyl groups. Without the methyl groups, the rigid side chains of the aromatic

Table 1 Experimental restraints and structural statistics

Number of experimental restraints	Unambiguous	Ambiguous
Distance restraints from NOEs		
Intramolecular (HP1β)	859	1,740
Intramolecular (peptide)	25	17
Intermolecular	30	188
Dihedral restraints[24] (HP1β)	22	
	⟨SA⟩	$\langle SA \rangle_c$
Coordinate precision*		
RMSD of backbone atoms (Å)	0.68 ± 0.07	0.54
RMSD of all heavy atoms (Å)	1.15 ± 0.08	1.07
RMS deviations		
From the experimental restraints		
NOE distances (Å)	0.018 ± 0.0047	0.024
Dihedral angles (°)	0.386 ± 0.106	0.331
From idealized geometry		
Bonds (Å)	0.002 ± 0.00014	0.0017
Angles (°)	0.366 ± 0.0082	0.372
Impropers (°)	0.248 ± 0.0154	0.260
Final energy, $E_{L\text{-}J}$ (kJ mol^{-1})†	−282.5 ± 17	−266.41
Ramachandran analysis		
Residues in most-favoured regions	74.1%	80.4%
Residues in additionally allowed regions	19.7%	17.9%
Residues in generously allowed regions	4.1%	0.0%
Residues in disallowed regions	2.1%	1.8%

⟨SA⟩ is the average root mean square (RMS) deviation for the ensemble; $\langle SA \rangle_c$ is the value for the structure that is closest to the mean. RMSD, RMS deviation. Confidence intervals are s.d.
*Computed over residues 19–71 of HP1β and 4–10 of the histone H3 peptide.
†The Lennard-Jones potential was not used at any stage in the refinement.

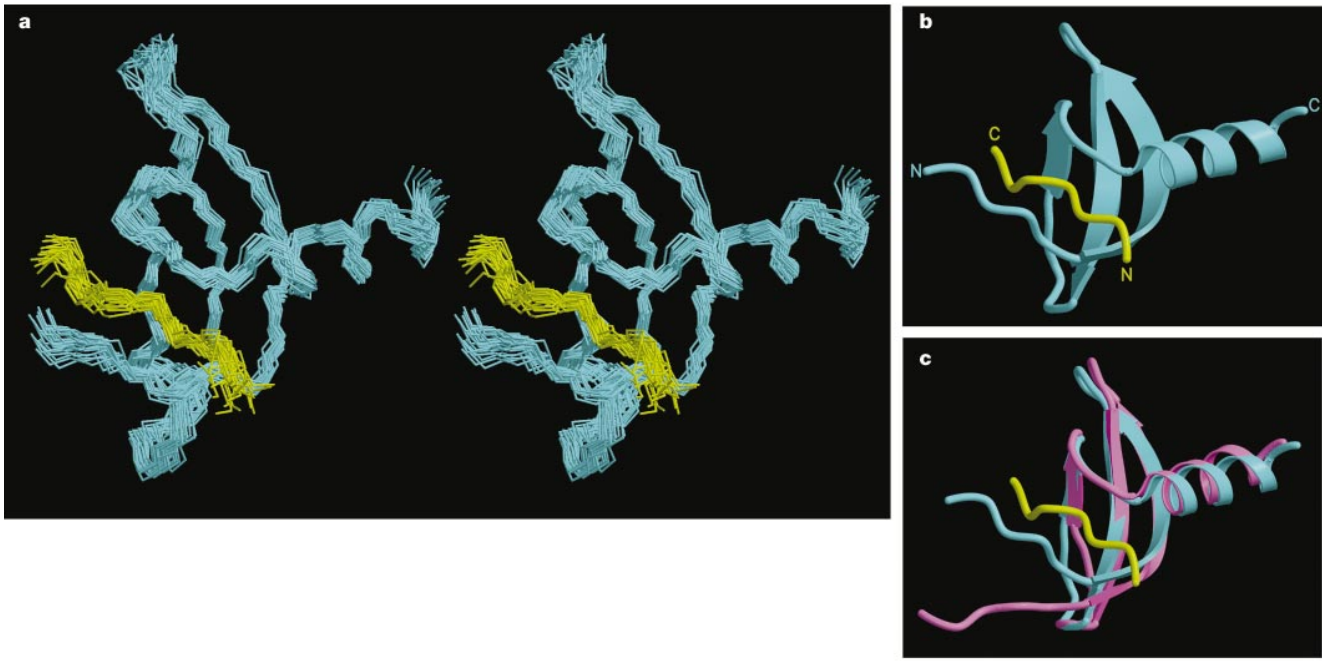

Figure 1 Structure of the HP1β chromodomain complexed with a histone H3 peptide dimethylated at lysines 4 and 9. **a**, Stereo view of the backbone of residues 19–71 of HP1β and 4–10 of histone H3 from the 25 lowest energy structures (of 75 that converged from the 100 computed). In the final structures no distance restraints were violated by more than 0.5 Å and no dihedral angle restraints by more than 5°. The structure has good covalent geometry and non-bonded contacts (Table 1). **b**, The structure closest to the mean in the same orientation as that shown in **a**. HP1β is blue and the histone H3 peptide is yellow. **c**, The structure closest to the mean overlaid with that of the free HP1β chromodomain[10] in pink. Figures 1 and 2 were generated using Molscript[25] and Raster 3D[26].

residues probably can not form the tight cluster that stabilizes the peptide-binding conformation. In contrast, more flexible aliphatic side chains would pack together without forming a pocket. Moreover, with aromatic residues interactions between π electrons and the positively charged nitrogen can contribute to the binding. This hypothesis is supported by the observation that the Y21L mutation significantly reduces peptide binding (data not shown). These aromatic residues are conserved in other chromodomains, as are Thr 51, which interacts with the Lys 9 side chain, and Glu 53 and Asn 57, which interact with the peptide backbone at the other end of the methyl lysine binding site (Fig. 2a). These two sets of residues thus define the methyl lysine binding site, which binds in an almost fully extended conformation along Trp 42 and Thr 51. Specificity is provided because no other hydrophobic side chain would be large enough to span the distance between the methyl-binding pocket and the backbone-binding site, and thus be able to substitute for methyl lysine (Fig. 2a).

The structure and proposed mechanism of methyl lysine recognition allows us to predict which chromodomain-like sequences adopt the same fold and probably bind peptides that contain methyl lysine (Fig. 3a). The residue at position 42 (invariably tryptophan) is in the hydrophobic core and is probably essential for the chromodomain fold. However, there are no specific structural requirements for aromatic residues at positions 21 and 45, although both are found in most chromodomains, including those of the HP1, the Suv39 and Pc-like families, chromomethylase, *Tetrahymena thermophila* Pdd1p, and other proteins (Fig. 3a). The other residues that interact with methyl lysine—Thr 51, Glu 53 and Asn 57 in HP1—are also generally conserved in this set of chromodomains, which supports our predictions (Fig. 3a). However, there are occasional, non-essential variations of these residues in some proteins, for example, N57D in the HP1 fission yeast homologue SWI6, which is known to bind Lys 9-methylated H3 (refs 2, 4). The sequences of the CHD proteins suggest that only the first of the pair of chromodomains in CHD1 and CHD2 could recognize methyl lysine, whereas neither of the chromodomains in CHD3 and CHD4 conform with the requirements for methyl lysine recognition (Fig. 3a).

In other chromodomains, which lack the complete set of conserved aromatic residues, there is no conservation of the other methyl lysine-interacting residues. Most of these sequences are compatible with the structural determinants of the chromodomain fold, including several proteins that have no known chromatin connection (Fig. 3a). The only exceptions are the 'RNA-binding chromodomains' from MSL3, MOF1 and related proteins[14]. These do not contain the methyl lysine-interacting residues, but they are also unlikely to adopt the canonical chromodomain fold because they lack principal conserved hydrophobic amino acids (Fig. 3a).

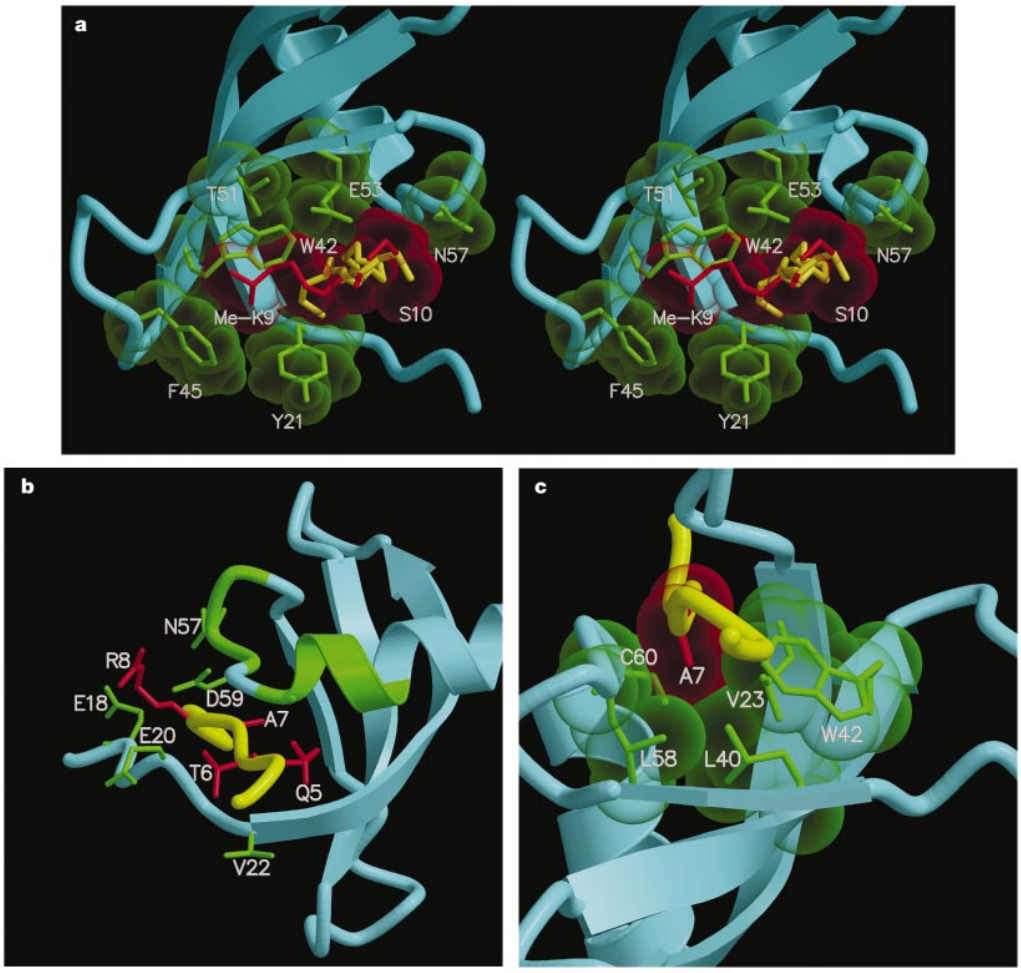

Figure 2 The interface between the chromodomain and the methylated peptide. **a**, Tyr 21, Trp 42 and Phe 45 form a 'hydrophobic box' that binds the *N*-methyl groups. The methyl lysine side chain binds along the surface of Trp 42 and Thr 51, whereas Glu 53 and Asn 57 contact the Cα end. **b**, Gln 5 interacts with the N terminus of the α-helix and Arg 8 interacts with a patch of acidic residues to help structure the flexible N-terminal tail. **c**, Ala 7 binds in the core of the chromodomain, making contacts with residues Val 23, Leu 40, Trp 42, Leu 58 and Cys 60. In **a**, **b** and **c**, side chains of the histone H3 peptide are red and interacting residues in the chromodomain are green.

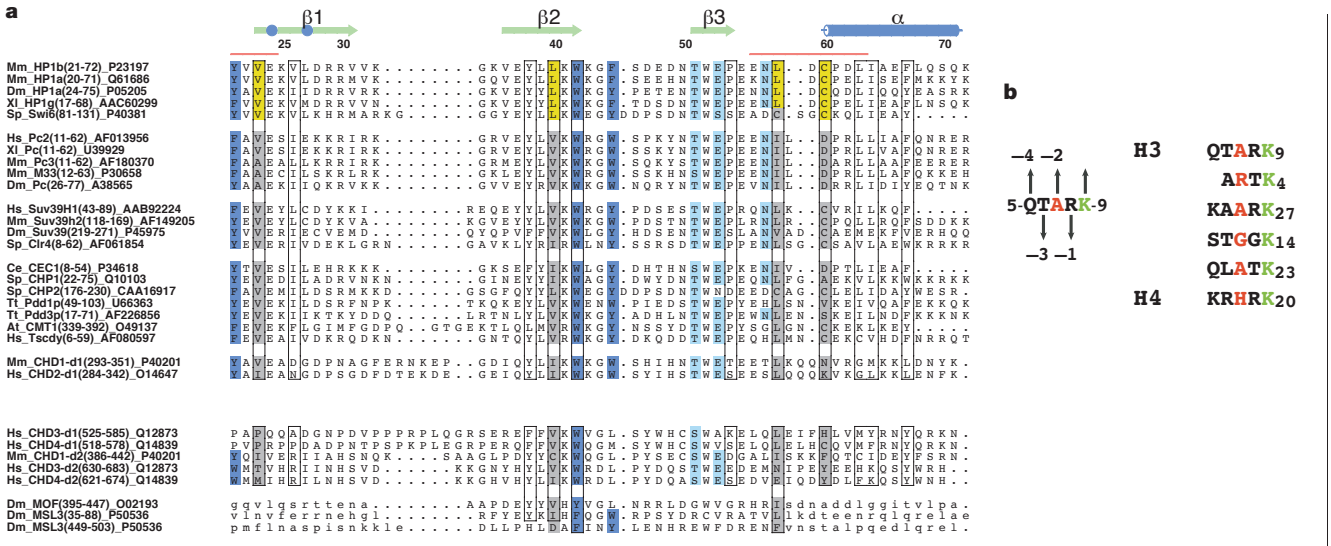

Figure 3 Sequence comparisons and residues involved in complex formation. **a**, Chromodomain alignment numbered for mouse HP1β. Residues important for methyl lysine recognition are blue (*N*-methyl groups) and light blue (Lys 9 side chain or backbone). Residues that make contacts with the K − 2 position of the peptide (see text) are shown in yellow (HP1 family) or grey (others). The two segments of HP1β that form the walls of the peptide-binding groove are indicated by red lines. β-strands are indicated by green arrows and the α-helix by a blue cylinder. The blue dots indicate the positions of conserved bulges in β1. Conserved hydrophobic residues that define the fold and the borders of the turn between the β-strand and the α-helix (Pro 54 and Cys 60, respectively) are boxed. The regions in MSL3 and MOF1 that do not conform with a canonical chromodomain fold are shown in small letters. Sequences are labelled by species name (Mm, *Mus musculus*; Dm, *Drosophila melanogaster*; Xl, *Xenopus laevis*; Hs, *Homo sapiens*; Sp, *Schizosaccharomyces pombe*; Ce, *Caenorhabditis elegans*; Tt, *Tetrahymena thermophila*; At, *Arabidopsis thaliana*), followed by protein name, residue range and GenBank accession number. Produced using Alscript[27]. **b**, The sequence of the N-terminal tail of histone H3. Up arrows denote side chains that point into the chromodomain core; down arrows denote surface side chains. The right panel shows the N-terminal histone H3 and H4 sequences aligned around the lysines. The key K − 2 position is shown in red and the lysines in green.

The HP1 chromodomain does not recognize methyl lysine as a free amino acid[15]. We also found that neither of its derivatives, 4-dimethylamino-butyric acid (pH 7.5) and 3-dimethylamino-1-propanol, altered the NMR spectra when added to the HP1β chromodomain (data not shown). The recognition of methyl lysine thus depends on the context in which it is presented. The peptide we used was dimethylated at both Lys 4 and Lys 9, but only the dimethyl group of Lys 9 is buried in the structure. Consistent with this, a Lys 9-methylated peptide binds as well (K_d 0.7 μM) as the Lys 4,9 bis-methylated peptide (K_d 1.9 μM). Moreover, the complexes have virtually identical NMR spectra. The structure thus confirms that methylation of Lys 4 neither contributes to nor interferes with recognition of methylated Lys 9.

The additional contacts to the chromodomain mainly involve the four amino acids that precede Lys 9: QTAR (Figs 2b and 3b). The structure allows us to propose a peptide motif that is recognized by the HP1 chromodomains. The side chain in the −2 position relative to methyl lysine (K − 2) seems to be central for specificity: Ala 7 is buried in a small hydrophobic pocket, formed by residues Val 23, Leu 40, Trp 42, Leu 58 and Cys 60, which are conserved in the HP1 family (Fig. 3a). Only alanine, or the smaller glycine, can be accommodated (Fig. 2c). Disruption of this binding site by mutation of Val 23 in *Drosophila* HP1 to the bulkier methionine abolishes binding of Lys 9-methylated H3 (refs 2, 3) and impairs its biological function[16]. At K − 4, Gln 5 interacts with the N terminus of the chromodomain α-helix (Fig. 2b). Here, positively charged residues would prevent binding owing to electrostatic repulsion by the helix dipole, whereas bulky hydrophobic residues will obstruct binding owing to interference with the hydration of the helix N terminus. The K − 1 and K − 3 side chains (Thr 6 and Arg 8) point away from the interaction surface. It is probable that any amino acid could be tolerated at these positions, but Arg 8 interacts with acidic residues in the flexible N-terminal tail (Fig. 2b) and probably contributes to binding.

Other lysines are methylated in histone tails, namely Lys 4 and Lys 27 in H3, and Lys 20 in H4 (Fig. 3b). Lys 4-methylated H3, which does not bind HP1, has an unacceptable arginine at K − 2, as does Lys 20-methylated H4 (histidine). Lys 27-methylated H3 has an acceptable alanine at K − 2, but an unfavourable positively charged and bulky lysine at K − 4. This explains why Lys 27-methylated H3 binds HP1 much more weakly, despite its similar sequence (data not shown). Of the other lysines, only Lys 14 and Lys 23 in H3 would present the modification in a suitable context for recognition by the HP1 chromodomain. However, neither is known to be methylated *in vivo*, although both can be acetylated.

Residues in HP1β that interact with Lys 9-methylated histone H3 are conserved in the HP1 family, for example, those interacting with Ala 7 (see above), but not in the other chromodomains. There is, however, conservation of the equivalent residues in separate chromodomain families and subfamilies, suggesting that each may recognize methyl lysine in a different, family-specific context (Fig. 3a). For example, the Pc-like chromodomains are likely to have a bigger pocket for the residue at K − 2. It is also possible that the binding of methyl lysine-containing peptides to other chromodomains might occur in the reverse orientation to that observed in HP1. If this were the case, the key positions for context recognition would be K + 2 and K + 4 rather than K − 2 and K − 4. As new methylation sites are identified, we will be able to refine our understanding of how protein methylation regulates chromodomain binding. □

Methods

Expression and purification of the HP1 chromo domain

Unlabelled, and ^{15}N- and ^{15}N/^{13}C-labelled mouse HP1β chromodomains (residues 10–80) were expressed and purified as described[11].

Synthetic peptides and binding assays

The synthetic N-terminal histone H3 peptides (NH_2-ARTK(Me)$_2$QTARK(Me)$_2$STGGKAPGG-COOH; NH_2-ARTK(Me)$_3$QTARK(Me)$_3$STGGKAPGG-COOH and NH_2-ARTKQTARK(Me)$_3$STGGKA-COOH) were synthesized and purified by G. Bloomberg. As judged by measurement of changes in the chromodomain's instrinsic tryptophan

fluorescence, these peptides bind with affinities of 2.14 ± 0.36, 1.94 ± 0.65 and 0.68 ± 0.05 μM, respectively.

Expression, purification and methylation of the peptide

Glutathione *S*-transferase (GST)–H3 (residues 1–13) was expressed in *Escherichia coli* BL21 cells and purified using standard protocols. The GST-fusion peptide was digested with thrombin and purified by reverse phase HPLC on an octadecyl (C_{18}) column using a buffer containing 0.1% trifluoroacetic acid in acetonitrile/water. The eluted peptide was freeze dried, dissolved in water and dimethylated as described[17] using a 20% ^{13}C-labelled formaldehyde (CIL)/water solution. The uniform methylation of the peptide was verified by mass spectrometry.

NMR spectroscopy

Purified chromodomain, after gel filtration chromatography, was concentrated to about 200 μl and mixed directly with histone H3 peptide to make NMR samples in 150 mM NaCl, 20 mM phosphate buffer (either pH 5.5 or 7.5), 10% D_2O. The peptide binds in fast exchange on the NMR timescale and spectra were recorded (at 25 °C on Bruker DRX600 and DRX800 spectrometers) using 2:1 and 0.9:1 (peptide:protein) ratios for assignment of the protein and peptide resonances, respectively. The protein backbone and side-chain resonances were assigned with standard triple-resonance NMR techniques[18] using a ^{13}C/^{15}N-labelled sample of HP1β chromodomain complexed with the unlabelled 18-residue histone H3 peptide. The peptide resonances were assigned using ^{13}C, ^{15}N-rejected nuclear Overhauser effect and total correlation spectroscopy (NOESY and TOCSY) experiments and the methyl group resonances of lysines 4 and 9 were confirmed with the help of a sample comprising an unlabelled chromodomain complexed to a selectively ^{13}C-methyl-labelled histone H3 peptide. NOEs were determined using two-dimensional NOESY and three-dimensional ^{13}C- and ^{15}N-separated NOESY spectra. Intermolecular contacts were obtained from a ^{13}C/^{15}N X-filtered NOESY spectrum[19] and a three-dimensional *J*(CH,NH)-separated NOESY spectrum[20]. Spectra were processed with the AZARA suite of programs (W. Boucher, unpublished) and analysed with ANSIG[21].

Structure determination

Structures were calculated from an extended template using simulated annealing in CNS version 1.0 (ref. 22) and ARIA[23], which uses the previous structures to identify restraint violations and removes ambiguous restraints that do not contribute sufficiently to the intensity of the peak. To generate the final NOE tables, nine iterations were calculated, each on 20 structures. Finally, 100 structures were calculated, from which the 25 with lowest energy were selected.

Received 9 January; accepted 7 February 2002.
Published online 20 February 2002, DOI 10.1038/nature722.

1. Strahl, B. D. & Allis, C. D. The language of covalent histone modifications. *Nature* **403,** 41–45 (2000).
2. Bannister, A. J. *et al.* Selective recognition of methylated lysine 9 on histone H3 by the HP1 chromo domain. *Nature* **410,** 120–124 (2001).
3. Lachner, M., O'Carroll, D., Rea, S., Mechtler, K. & Jenuwein, T. Methylation of histone H3 lysine 9 creates a binding site for HP1 proteins. *Nature* **410,** 116–120 (2001).
4. Nakayama, J., Rice, J. C., Strahl, B. D., Allis, C. D. & Grewal, S. I. Role of histone H3 lysine 9 methylation in epigenetic control of heterochromatin assembly. *Science* **292,** 110–113 (2001).
5. Zhang, Y. & Reinberg, D. Transcription regulation by histone methylation: interplay between different covalent modifications of the core histone tails. *Genes Dev.* **15,** 2343–2360 (2001).
6. Rea, S. *et al.* Regulation of chromatin structure by site-specific histone H3 methyltransferases. *Nature* **406,** 593–599 (2000).
7. Noma, K., Allis, C. D. & Grewal, S. I. Transitions in distinct histone H3 methylation patterns at the heterochromatin domain boundaries. *Science* **293,** 1150–1155 (2001).
8. Litt, M. D., Simpson, M., Gaszner, M., Allis, C. D. & Felsenfeld, G. Correlation between histone lysine methylation and developmental changes at the chicken β-globin locus. *Science* **293,** 2453–2455 (2001).
9. Nielsen, S. J. *et al.* Rb targets histone H3 methylation and HP1 to promoters. *Nature* **412,** 561–565 (2001).
10. Ball, L. J. *et al.* Structure of the chromatin binding (chromo) domain from mouse modifier protein 1. *EMBO J.* **16,** 2473–2481 (1997).
11. Brasher, S. V. *et al.* The structure of mouse HP1 suggests a unique mode of single peptide recognition by the shadow chromo domain dimer. *EMBO J.* **19,** 1587–1597 (2000).
12. Horita, D. A., Ivanova, A. V., Altieri, A. S., Klar, A. J. & Byrd, R. A. Solution structure, domain features, and structural implications of mutants of the chromo domain from the fission yeast histone methyltransferase Clr4. *J. Mol. Biol.* **307,** 861–870 (2001).
13. Cowieson, N. P., Partridge, J. F., Allshire, R. C. & McLaughlin, P. J. Dimerisation of a chromo shadow domain and distinctions from the chromodomain as revealed by structural analysis. *Curr. Biol.* **10,** 517–525 (2000).
14. Akhtar, A., Zink, D. & Becker, P. B. Chromodomains are protein–RNA interaction modules. *Nature* **407,** 405–409 (2000).
15. Jacobs, S. A. *et al.* Specificity of the HP1 chromo domain for the methylated N-terminus of histone H3. *EMBO J.* **20,** 5232–5241 (2001).
16. Platero, J. S., Hartnett, T. & Eissenberg, J. C. Functional analysis of the chromo domain of HP1. *EMBO J.* **14,** 3977–3986 (1995).
17. Means, G. E. & Feeney, R. E. Reductive alkylation of amino groups in proteins. *Biochemistry* **7,** 2192–2201 (1968).
18. Ferentz, A. E. & Wagner, G. NMR: A multifaceted approach to macromolecular structure. *Q. Rev. Biophys.* **33,** 29–65 (2000).
19. Zwahlen, C. *et al.* Methods for measurement of intermolecular NOEs by multinuclear NMR spectroscopy: Application to a bacteriophage λ N-peptide/boxB RNA complex. *J. Am. Chem. Soc.* **119,** 6711–6721 (1997).
20. Melacini, G. Separation of intra- and intermolecular NOEs through simultaneous editing and J-compensated filtering: A quadrature-free constant-time J-resolved approach. *J. Am. Chem. Soc.* **122,** 9735–9738 (2000).
21. Kraulis, P. J. *et al.* The solution structure and dynamics of ras p21.GDP determined by heteronuclear three- and four-dimensional NMR spectroscopy. *Biochemistry* **33,** 3515–3531 (1994).
22. Brunger, A. T. *et al.* Crystallography and NMR system (CNS): A new software system for macromolecular structure determination. *Acta Crystallogr. D* **54,** 905–921 (1998).
23. Linge, J. P., O'Donoghue, S. J. & Nilges, M. Automated assignment of ambiguous NOEs with ARIA. *Methods Enzymol.* **339,** 71–90 (2001).
24. Cornilescu, G., Delaglio, F. & Bax, A. Protein backbone angle restraints from searching a database for chemical shift and sequence homology. *J. Biol. NMR* **13,** 289–302 (1999).
25. Kraulis, P. J. MOLSCRIPT: a program to produce both detailed and schematic plots of protein structures. *J. Appl. Crystallogr.* **24,** 946–950 (1991).
26. Merrit, E. A. & Murphy, M. E. P. Raster3D Version 2.0. A program for photorealistic molecular graphics. *Acta Crystallogr. D* **50,** 869–873 (1994).
27. Barton, G. J. ALSCRIPT: a tool to format multiple sequence alignments. *Protein Eng.* **6,** 37–40 (1993).

Acknowledgements

We thank A. Verreault for the pGEX-H3 construct; R. Turner, P. Sharratt and the PNAC facility for mass spectrometry and amino-acid analysis; A. Thiru for comments on the manuscript; the Medical Research Council for a Career Development Award (to H.R.M.); and the Wellcome Trust for financial support. The Cambridge Centre for Molecular Recognition is supported by the Biotechnology and Biological Sciences Research Council and the Wellcome Trust.

Competing interests statement

The authors declare that they have no competing financial interests.

Correspondence and requests for material should be addressed to N.V.M. (e-mail: nm@mole.bio.cam.ac.uk) or E.D.L. (e-mail: e.d.laue@bioc.cam.ac.uk). The coordinates have been deposited in the Protein Data Bank under accession number 1GUW.